

STATCOM controller design for power system stabilization with sub-optimal control and strip pole assignment

Yuang-Shung Lee*, San-Yung Sun

Department of Electronic Engineering, Fu-Jen Catholic University, 510 Chung-Cheng Road, Hsin-Chuang, Taipei 24205, Taiwan, ROC

Received 8 September 2000; revised 3 January 2001; accepted 16 October 2001

Abstract

This paper solves the problem of power system stabilization by using the advanced static VAR compensator (STATCOM) to increase the damping of the electromechanical and exciter modes of the power system. The dynamic oscillations are repressed by the proposed STATCOM controller, which is designed using a two-level optimization output feedback control and the strip poles assignment method. The linear quadratic regulator method does not require pre-specified weighting matrices. The two output feedback control schemes, designed using the direct and minimum error excitation methods, respectively, are compared. To show the effectiveness of the dynamic oscillation suppression, eigenvalue analysis and nonlinear simulation were used to demonstrate that the proposed STATCOM controller significantly improves the dynamic performance of the power system. © 2002 Elsevier Science Ltd. All rights reserved.

Keywords: STATCOM; Strip pole assignment; Minimum error excitation; Power system stabilization

1. Introduction

Due to the increase in power requirements, it is important to supply power more effectively. High voltage DC transmission provides improved power transmission for networks. The flexible AC transmission system (FACTS) is a conventional AC transmission system with added power electronic conditioners for greater efficiency. Advanced static VAR compensator (STATCOM) is one of the FACTS equipment packages. In 1992, an 80 MVA static VAR generator (SVG) was developed for industry by Japan. This was a proof that the SVG can increase system damping, power system stabilization, and power transmission limits. In 1994, the biggest SVG was equipped in the United States. This unit decreased low frequency oscillation and made the voltage more stable [1].

In a power system, oscillations occur when there are disturbances in the system such as a change in load or a fault in the system. The damping of the system should be great enough that the synchronous generators can return to a steady state after disturbances [2]. These oscillations can injure the power transmission. Several studies have provided various methods for oscillation damping, such as excitation control [3], static VAR compensator (SVC)

[4–6], the NGH scheme [7], static phase-shifters [8] and superconducting magnetic energy storage (SMES) [9,10], etc. STATCOM is a second generation FACTS equipment based on a voltage source inverter. The major advantages of STATCOM over the conventional SVC are, significant size reduction and reduced number of passive elements due to the development of supercapacitor technology and the ability to supply required reactive power even at low bus voltages [11].

This study examined the application of STATCOM for damping electromechanical oscillation in a power system. We considered a power system with static and dynamic loads. When a disturbance occurs, the STATCOM controller can provide a damping torque signal to improve the system stabilization to make the system return to a steady state quickly, make the system damping large enough to decrease the oscillations, and pre-specify the system eigenvalues to a stable range for the desired relative stability. The output feedback controller can be used to design a STATCOM controller for damping system oscillations under the structure constrained in a practical system.

2. System model

This power system consists of a synchronous generator connected to two parallel lines through a single line to the infinite bus. A static, dynamic load and a STATCOM unit

* Corresponding author. Tel.: +886-2-2903-1111x3791; fax: +886-2-2904-2638.

E-mail address: lee@ee.fju.edu.tw (Y.-S. Lee).

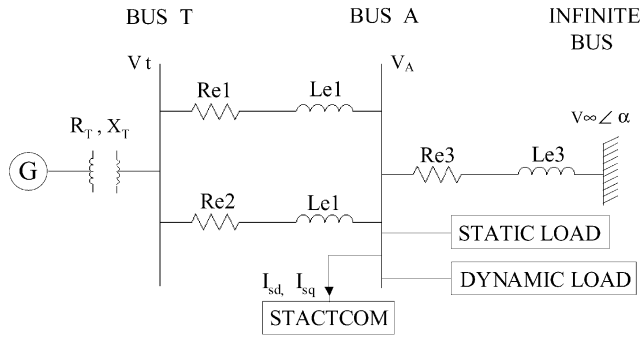


Fig. 1. System model.

are located at the load bus, as shown in Fig. 1. The dynamic generator equation can be described as a two-axis model [2], where the transient voltage equations are

$$\dot{E}'_d = [-E'_d - (X_q - X'_d)I_q]/T'_{q0} \quad (1)$$

$$\dot{E}'_q = [E_{FD} - E'_q + (X_d - X'_d)I_d]/T'_{d0} \quad (2)$$

The swing equations are

$$\dot{\omega} = (P_m - D_g\omega - P_e)/M_g \quad (3)$$

$$\dot{\delta} = \omega_b(\omega - 1) \quad (4)$$

where $P_e = E'_d I_d + E'_q I_q$ is the electromagnetic power of the generator.

The system excitation for the synchronous generator was selected as the IEEE Type-1 excitation system with a constant prime mover mechanical torque, and a *s*-domain block, as shown in Fig. 2 [12].

The static load is generally represented by voltage dependent nonlinear functions. The load equations which describe the active and reactive power are [13–15]

$$P_L = c_p V_A^{n_p} \quad Q_L = c_q V_A^{n_q} \quad (5)$$

where the weighted coefficient percentages c_p and c_q describe the amount of power. The exponents, n_p and n_q , identify the load characteristics and are usually determined using measured load mixed data for the load buses.

The dynamic load is constructed by a group of induction motors [15–17]. For stability study purposes, these motors

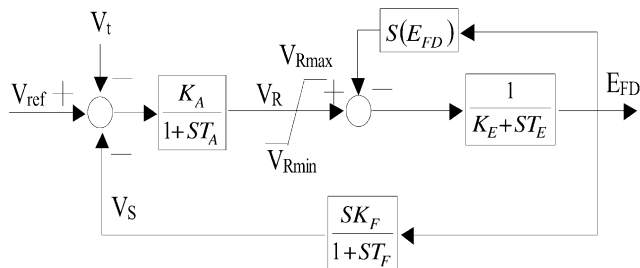


Fig. 2. Exciter.

can be combined into an equivalent one using the aggregation method [18]. A fifth-order dynamic model of the induction motor was used in this study to obtain a more detailed result. The dynamic equations are

$$\frac{d}{dt}[I] = [L]^{-1}\{-[R][I] + [V]\} \quad (6)$$

$$\frac{d\omega_r}{dt} = (T_{me} - T_{mm})/2H_m \quad (7)$$

where

$$[I] = [I_{qsm} \quad I_{dsm} \quad I_{qrm} \quad I_{dr}]^T$$

$$[V] = [V_{qA} \quad V_{dA} \quad 0 \quad 0]^T$$

$$[L] = \begin{bmatrix} L_{SS} & 0 & L_M & 0 \\ 0 & L_{SS} & 0 & L_M \\ L_M & 0 & L_{Tr} & 0 \\ 0 & L_M & 0 & L_{Tr} \end{bmatrix}$$

$$[R] = \begin{bmatrix} R_S & -\omega L_{SS} & 0 & -\omega L_M \\ \omega L_{SS} & R_S & \omega L_M & 0 \\ 0 & -(\omega - \omega_r)L_M & R_r & -(\omega - \omega_r)L_{Tr} \\ (\omega - \omega_r)L_M & 0 & (\omega - \omega_r)L_{Tr} & R_r \end{bmatrix}$$

$$T_{me} = L_M(I_{dsm}I_{qrm} - I_{dr}I_{qsm})$$

The STATCOM unit configuration, as shown in Fig. 3, contains a $Y-\Delta/Y-Y$ connected transformer, a 12-pulse cascaded bridge type converter/inverter, and a capacitor bank parallel with the leakage resistance. The forced-commutated GTO converter/inverter controls the firing angles θ_s of the cascaded converter/inverter and provides the STATCOM with the ability to control the reactive power flow in the three-phase AC bus.

The STATCOM mathematical model can be written with

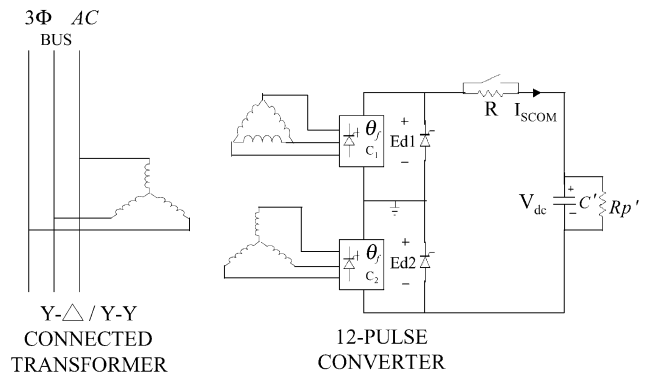


Fig. 3. Schematic configuration of STATCOM unit.

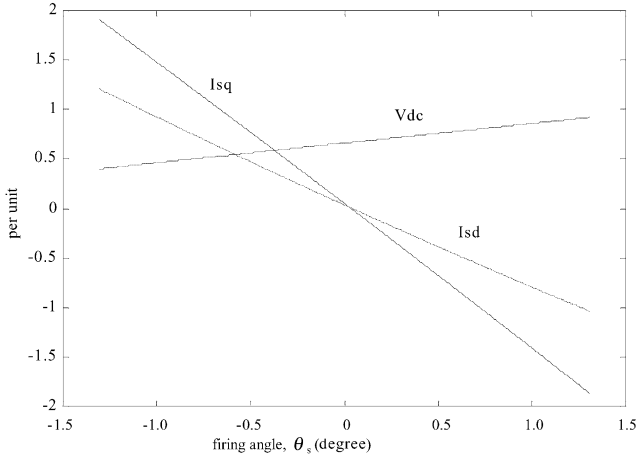


Fig. 4. STATCOM steady state performance.

the I_{sd} , I_{sq} , and V_{dc} differential equation in the form [19]

$$\dot{I}_{sd} = \frac{-R'_s \omega_b}{L'} I_{sd} - \omega I_{sq} + \frac{K \omega_b}{L'} \cos(\theta_s) V_{dc} - \frac{\omega_b}{L'} V_{dA} \quad (8)$$

$$\dot{I}_{sq} = \omega I_{sd} - \frac{R'_s \omega_b}{L'} I_{sq} + \frac{K \omega_b}{L'} \sin(\theta_s) V_{dc} - \frac{\omega_b}{L'} V_{qA} \quad (9)$$

$$\begin{aligned} \dot{V}_{dc} = & -\frac{3}{2} KC' \omega_b \cos(\theta_s) I_{sd} \\ & - \frac{3}{2} KC' \omega_b \sin(\theta_s) I_{sq} - \frac{\omega_b C'}{R_p} V_{dc} \end{aligned} \quad (10)$$

where I_{sd} and I_{sq} are the active and reactive current flows in/out bus A, and V_{dc} is the voltage of the capacitor. The steady state characteristics of the three states of the STATCOM model are plotted in Fig. 4 as a function of the firing

angle θ_s . It can be seen that the three states are nearly linear around the operation point.

Combining the generator, excitor, and loads, we can obtain a set of 12th-order nonlinear differential equations. The system data are given in Appendix A. At the initial operating point, all of the nonlinear differential equations can be linearized to obtain linear differential state equations. The stability of the system can be determined by examining the eigenvalues obtained from those linear state equations. All of the eigenvalues must be located at a distance from the imaginary axis for better system damping.

The complete eigenvalues for the open-loop system, without the STATCOM unit, are tabulated in the second column of Table 1. The electromechanical mode and exciter mode are located at $-0.302 \pm j9.632$ and $-0.987 \pm j1.193$, respectively. It is observed that there is very low damping on the low frequency oscillation, which is dominantly affected by the electromechanical mode. When the STATCOM unit is incorporated into the power system, the system eigenvalues are given in the third column of Table 1; the electromechanical mode is still not sufficient. Therefore, some additional control signals must be employed to repress the low frequency oscillation under system disturbances.

3. STATCOM controller design

3.1. Strip-eigenvalue assignment

In this paper, a supplementary STATCOM controller is proposed to increase the damping of the electromechanical mode. The bus voltage V_A feedback is used to regulate the reactive power to damp the system voltage stability. Applying the state feedback and output feedback as the damping signal, the STATCOM controller can provide a supplementary damping signal to the

Table 1
System eigenvalues

| | Without STATCOM | With STATCOM but without controller | With STATCOM and state feedback | With STATCOM and output feedback | |
|-----------------|------------------------|-------------------------------------|---------------------------------|----------------------------------|-------------------------|
| | | | | By direct method | By MEE method |
| Generator | $-1.918 \pm j2.846$ | $-2.039 \pm j2.939$ | $-2.039 \pm j2.939$ | $-0.851 \pm j2.468$ | $-1.459 \pm j2.278$ |
| | $-0.302 \pm j9.632^a$ | $-0.304 \pm j9.467^a$ | $-2.264 \pm j9.383^a$ | $-2.820 \pm j9.562^a$ | $-2.276 \pm j9.401^a$ |
| Exciter | -43.124 | -45.187 | -45.187 | -48.427 | -36.223 |
| | $-0.987 \pm j1.193^b$ | $-0.873 \pm j1.112^b$ | $-1.436 \pm j1.096^b$ | $-2.044 \pm j1.111^b$ | $-1.435 \pm j1.509^b$ |
| Induction motor | $-43.146 \pm j391.285$ | $-44.527 \pm j389.513$ | $-44.527 \pm j389.513$ | $-43.640 \pm j389.621$ | $-44.947 \pm j390.530$ |
| | $-10.249 \pm j30.612$ | $-10.249 \pm j30.098$ | $-10.249 \pm j30.098$ | $-10.048 \pm j29.846$ | $-10.268 \pm j30.201$ |
| | -14.758 | -15.650 | -15.650 | -15.738 | -15.614 |
| STATCOM | | $-212.550 \pm j47.581$ | $-212.550 \pm j47.581$ | -255.550 | -224.540 |
| | | $-73.014 \pm j1466.687$ | $-73.014 \pm j1466.687$ | -137.807 | -193.327 |
| | | | | $-71.740 \pm j1462.543$ | $-72.654 \pm j1472.289$ |

^a Electromechanical mode.

^b Exciter mode.

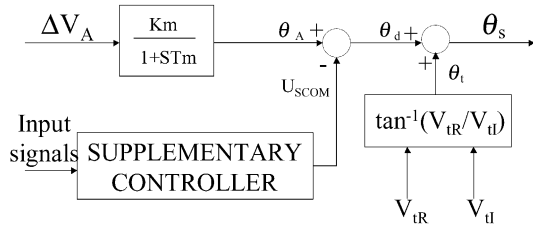


Fig. 5. STATCOM controller.

firing circuit input of the STATCOM unit, as shown in Fig. 5.

In order to determine the gain of the STATCOM controller, the linearized state equations of the system, including generator, exciter, loads, and STATCOM unit, are represented in the following compact form

$$\dot{X}(t) = AX(t) + BU(t), \quad X(t_0) = X_0 \quad (11)$$

$$Y(t) = CX(t) \quad (12)$$

where

$$X(t) = [\Delta\omega, \Delta\delta, \Delta V_{RE}, \Delta E_{FD}, \Delta V_s, \Delta E'_d, \Delta E'_q, \Delta I_{qsm}, \Delta I_{dsm},$$

$$\Delta I_{qrm}, \Delta I_{drn}, \Delta\omega_r, \Delta I_{sd}, \Delta I_{sq}, \Delta V_{dc}, \Delta\theta_A]^T$$

is the system state vector, $Y(t) = CX(t)$ is the output vector, $U(t) = U_{SCOM}$ is the supplementary control signal from the STATCOM controller. A , B , and C are the coefficient matrices of the system with an appropriate dimensions.

In the design of a conventional optimal control system, it is desired to get $U(t)$ such that the performance index J is minimum, where

$$J = \frac{1}{2} \int_0^{\infty} [X^T(t)QX(t) + U^T(t)RU(t)]dt \quad (13)$$

The weighting matrices Q and R are $n \times n$ nonnegative and $m \times m$ positive definite symmetrical matrices, respectively. The optimal control vector is $U^o(t) = -F^o X(t)$, where the feedback gain is $F^o = R^{-1}B^T K$ with K being a symmetric positive definite solution of the matrix form Riccati equation in closed form

$$A^T K + KA - KBR^{-1}B^T K + Q = 0_n \quad (14)$$

and the closed loop eigenvalues, denoted by $\Lambda(A - BF^o) = [\lambda_1, \dots, \lambda_m, \lambda_{m+1}, \dots, \lambda_n]$, will lie in the open left-half plane of the complex s -plane as the desired damping for the system.

In conventional LQR problems, the optimal gain is designed by selecting weighting matrices redundantly in accordance with the desired practical application. For simplicity, the matrices Q and R are usually chosen as dia-

gonal matrices. To improve the system performance, the weighting matrix R is set as an identity matrix for equal weighting of the m control inputs. The weighting matrix Q must be determined previously, such that the controlled eigenvalues λ_1 to λ_n will be selected and shifted to a desired location.

For a large-scale system, it is difficult to pre-determine the weighting matrices, Q and R . The repetitive trial-and-error method is the most common approach for determining the weighting matrices. To overcome this difficulty, a unified countermeasure is proposed as follows, where the closed-loop eigenvalues are shifted to a pre-specified vertical strip without the need for weighting matrices.

Let $\xi \geq 0$ be a real number, which represents the prescribed degree of relative stability. We change the system matrix to $\bar{A} = A + \xi I_n$, and the unstable system eigenvalues of \bar{A} will be shifted to their corresponding locations with respect to the $-\xi$ vertical line, where I_n is an identity matrix. The overall system eigenvalues of the closed loop system, $A_c = A - BR^{-1}B^T \bar{K}$, are on the left side of the $-\xi$ vertical line of the complex s -plane, where \bar{K} is the solution for the following closed form Riccati equation with $Q = 0_n$ [20]:

$$\bar{A}^T \bar{K} + \bar{K} \bar{A} - \bar{K} B R^{-1} B^T \bar{K} + Q = 0_n \quad (15)$$

Assume that ξ_1 and ξ_2 are two positive real numbers denoting the vertical strip of $[-\xi_2, -\xi_1]$ on the negative real axis of the complex s -plane. Given $\bar{A} = A + \xi_1 I_n$, the control law is modified to $U(t) = -\tilde{F}^o X(t) = -\rho \tilde{F} X(t) = -\rho R^{-1} B^T \tilde{K} X(t)$, where \tilde{F}^o is the optimal gain vector determined by the strip pole assignment method, matrix \tilde{K} is the solution for the modified Riccati equation:

$$\tilde{A}^T \tilde{K} + \tilde{K} \tilde{A} - \tilde{K} B R^{-1} B^T \tilde{K} = 0_n \quad (16)$$

The gain ρ is selected by

$$\rho = 0.5 \left(1 + \frac{\xi_2 - \xi_1}{\text{tr}(\tilde{A}^+)} \right) = 0.5 + \frac{\xi_2 - \xi_1}{\text{tr}(B \tilde{F}^+)} \quad (17)$$

where $\text{tr}(\tilde{A}^+) = -\sum_{i=1}^{n^+} \lambda_i^+ = 1/2 \text{tr}(B \tilde{F}^+)$ and λ_i^+ ($i = 1, \dots, n^+$) are the unstable eigenvalues of \tilde{A} .

The optimal closed-loop system become $\dot{X}(t) = (A - \rho B \tilde{F}) X(t)$, $\Lambda(A - \rho B \tilde{F})$ which denotes a set of eigenvalues located inside the vertical strip of $[-\xi_2, -\xi_1]$. As mentioned in Eq. (16) for equal m control input weighting, R can be a unity matrix. The proposed optimal strip eigenvalue placement can be used to design the supplementary damping controller without the need for weighting matrix Q .

3.2. Output feedback controller

Since the control signal from the optimal controller is

a linear time-invariant combination of all states, it is impractical in a real system. Some system states cannot be measured. Consequently, we want an output feedback controller with measurable signals:

$$U^S(t) = -P^S Y(t) = -P^S C X(t) = -F^S X(t) \quad (18)$$

It is noted that $U^S(t)$ is also a linear time-invariant combination of the system states and a near optimal controller.

3.2.1. Directed method

Let $F^S = \rho \tilde{F}$, then the output feedback gain designed by the directed method can be obtained from Eq. (18). The output feedback gain vector is

$$P^S = F^S C^+ = \rho \tilde{F} C^+ \quad (19)$$

where C^+ is the pseudo-inverse of matrix C . If there is only some feedback signal same as the states of the system, the output feedback gains are same as the state feedback gains which correspond to the measurable states.

3.2.2. Minimum error excitation method

If $F^S = \tilde{F}^o = \rho \tilde{F}$, the near optimal controller is optimal. However, this rarely occurs in practical systems. Therefore, we defined the state error vector

$$e(t) = X^S(t) - X^o(t), \quad e(t_0) = 0 \quad (20)$$

where $X^S(t)$ is the sub-optimal state vector, and $X^o(t)$ is the optimal state vector. Differentiating both sides of Eq. (20), and substituting Eq. (11) in Eq. (20), we get

$$\dot{e}(t) = (A - BF^S)e(t) + B(F^S - \tilde{F}^o)X^o(t) \quad (21)$$

Let the excitation error vector be

$$h(t) = (F^S - \tilde{F}^o)X^o(t); \quad (22)$$

then

$$\dot{e}(t) = (A - BF^S)e(t) + Bh(t), \quad e(t_0) = 0 \quad (23)$$

To minimize the effect of $h(t)$ in the time span, a quadratic excitation performance index \tilde{J} is defined as follows:

$$\tilde{J} = \frac{1}{2} \int_0^\infty h^T(t) \tilde{R} h(t) dt \quad (24)$$

Minimizing the excitation performance index yields the output feedback sub-optimal controller in Eq. (18) [21], where P^S is the output feedback gain and

$$P^S = \tilde{F}^o L C^T (C L C^T)^{-1} \quad (25)$$

L is the solution of the matrix equation

$$(A - B\tilde{F}^o)L + L(A - B\tilde{F}^o)^T = -I \quad (26)$$

The closed loop system with the output feedback sub-optimal controller is

$$\dot{X}(t) = (A - BF^S)X(t), \quad X(t_0) = X_0 \quad (27)$$

The output feedback controller designed using the second optimization approach only guarantees a minimum excitation performance index, but does not ensure a stable system. It is necessary to check that all eigenvalues of $(A - BF^S)$ have negative real parts and the pre-determined modes have adequate damping.

4. Results and simulations

Eigenvalue analysis is usually employed to investigate the small signal stability of a system. The pole configurations are utilized to verify the amplitude and the location of the dynamic modes of the studied system. The results are tabulated in Table 1, and the corresponding pole configuration is shown in Fig. 6. To improve the electromechanical modes damping of the studied system, we selected $[-\zeta_2, -\zeta_1] = [-4.1, -1.1]$ to design the STATCOM controller under two different control schemes as follows. The output vector $Y = [\Delta\omega, \Delta\delta, \Delta V_t, \Delta I_a]$ is chosen for this study.

Scheme A: optimal STATCOM controller designed using the optimal strip eigenvalue assigned method.

$$\begin{aligned} U_{\text{SCOM}}^S(t) = & -10.855\Delta\omega - 0.040\Delta\delta - 0.039\Delta V_{\text{RE}} \\ & - 0.050\Delta E_{\text{FD}} + 0.337\Delta V_s + 0.011\Delta E'_d \\ & - 0.402\Delta E'_q - 0.111\Delta I_{\text{qsm}} + 0.0002\Delta I_{\text{dsm}} \\ & - 0.113\Delta I_{\text{qrm}} + 0.00004\Delta I_{\text{drn}} - 0.053\Delta\omega_r \\ & - 0.001\Delta I_{\text{sd}} - 0.002\Delta I_{\text{sq}} + 0.001\Delta V_{\text{dc}} \\ & + 0.012\Delta\theta_A \end{aligned}$$

Scheme B: output feedback controller designed using the direct method. The feedback gain is the same as optimal feedback gain with the directed measurable state.

$$U_{\text{SCOM}}^d(t) = -10.855\Delta\omega + 0.175\Delta\delta - 0.229\Delta V_t - 0.190\Delta I_a$$

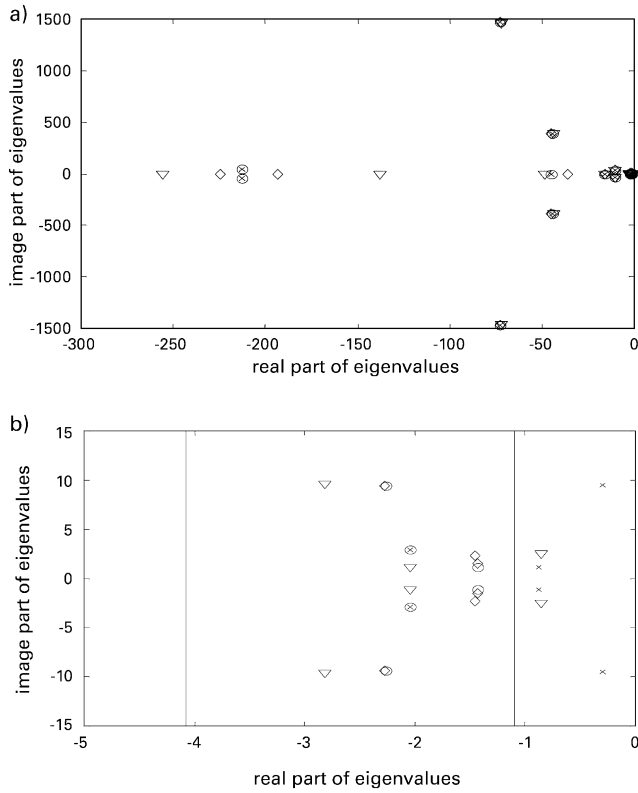


Fig. 6. Pole configuration of the studied system. (a) Pole configuration of all systems. (b) Pole configuration of the system from between $[-5,0]$. \times : system with STATCOM but without controller; \circ : system with STATCOM and state feedback controller; ∇ : system with STATCOM and output feedback controller (direct); \diamond : system with STATCOM and output feedback controller (MEE).

Scheme C: output feedback controller designed using the minimum error excitation method.

$$U_{SCOM}^m(t) = -8.669\Delta\omega - 0.049\Delta\delta - 0.518\Delta V_t + 0.040\Delta J_a$$

The eigenvalues of the system with the proposed opti-

mal STATCOM controller are tabulated in the fourth column of Table 1. The pole configurations are plotted in Fig. 6. It is observed that all of the eigenvalues are shifted to the vertical strip in $[-4.1, -1.1]$. The electromechanical mode and exciter mode shifts to $-2.264 \pm j9.383$ and $-1.436 \pm j1.096$, respectively. The damping ratio of the dominant mode can be improved to the pre-specified level for the desired system. It should be noted that the optimal STATCOM controller does not destroy the other mode shapes in the system. The eigenvalues with the output feedback excitation controller are given in the fifth and sixth columns of Table 1. The poles are also plotted in Fig. 6. The damping effect of the output feedback scheme is little smaller than that for the state feedback scheme, but the eigenvalues of the electromechanical mode and exciter mode are also near the vertical strip. The output feedback controller was designed using the minimum error excitation method. The system mode shapes were destroyed somewhat more than those in the state feedback scheme. The damping effects are as acceptable as the original state feedback control scheme. The minimum excitation error method is better than the direct method.

To examine the damping effect of the proposed controller during a dynamic period, we performed time domain simulations based on the nonlinear differential equations, which describe the system behavior under disturbance conditions. The nonlinearity, such as exciter ceiling voltage limit, must be included. A 100 ms, transmission line 1 open-fault was used as the power system disturbance. The dynamic responses of the power system are shown in Figs. 7–9. Fig. 7 shows the dynamic responses of the system under various controllers. Fig. 8 shows the dynamic responses of the system with the STATCOM controller, which was designed using the MEE method. Fig. 9 is the dynamic responses under

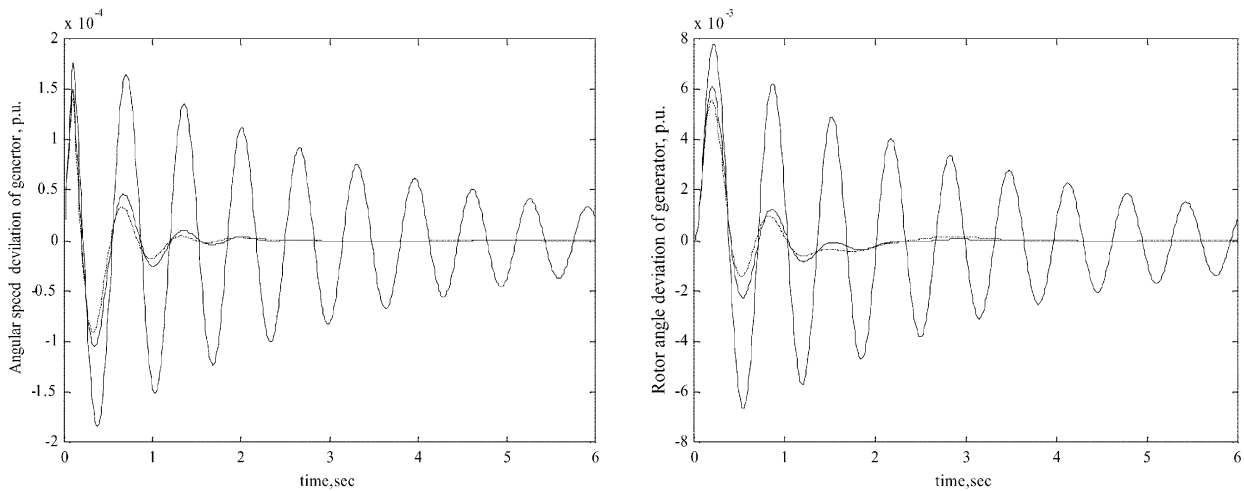


Fig. 7. Dynamic responses of the system for 100 ms, 1% mechanical torque change of generator. - - -: open system, - . - . -: System with STATCOM and output feedback controller (direct), system with STATCOM and output feedback controller (MEE).

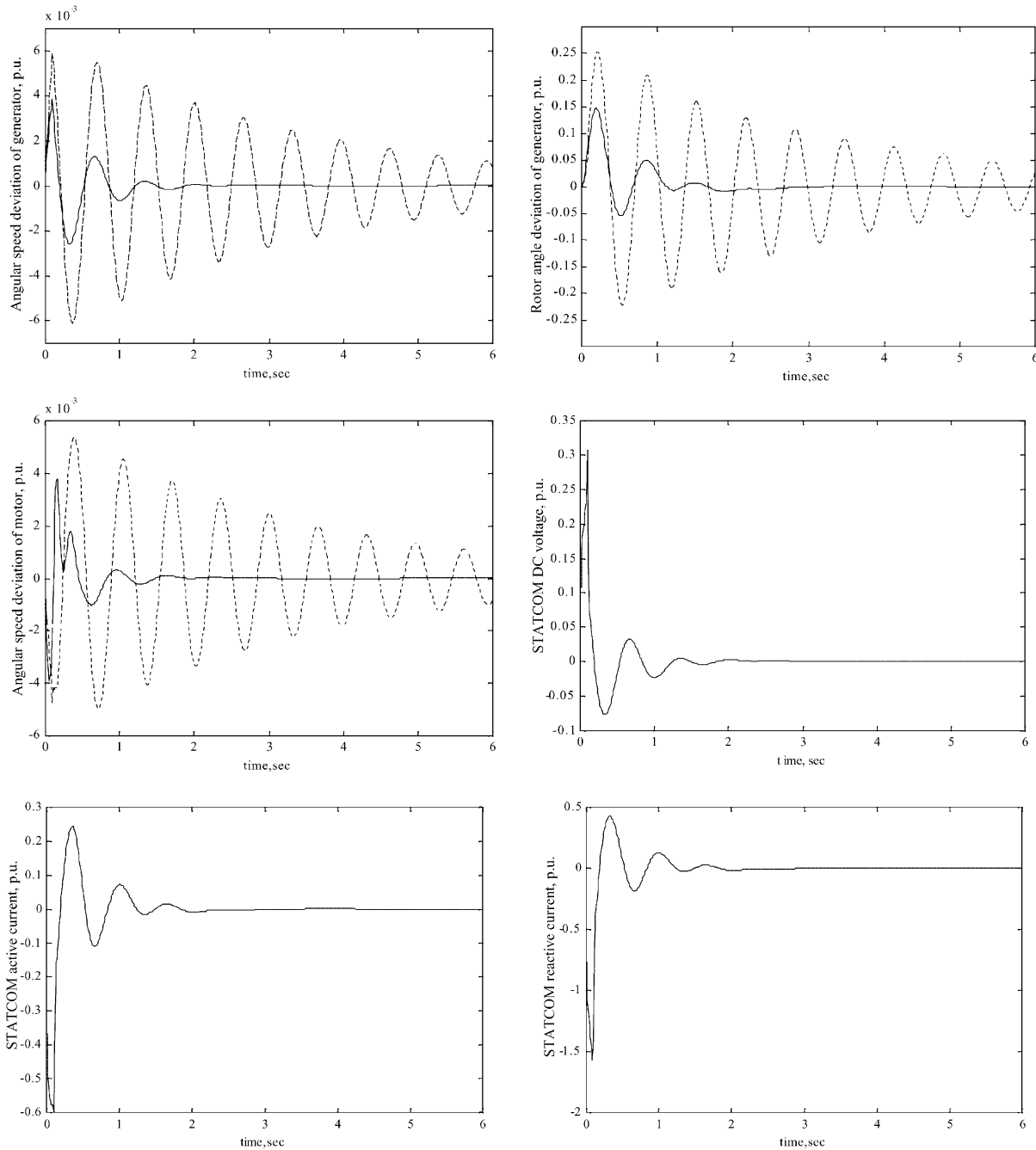


Fig. 8. Dynamic responses of the system for 100 ms, line open-fault disturbance. - - -: open system, —: system with STATCOM and output feedback controller (MEE).

various load conditions. The significant observations are summarized as follows:

1. The system with the optimal STATCOM controller can shift the electromechanical and exciter modes to a pre-specified vertical strip without affecting the other modes.
2. The systematic design method is very simple and does not involve weighting matrix pre-specification.
3. The sub-optimal STATCOM controller used only the available states as the feedback signals. The minimum error excitation method is better than the direct method because it does not destroy the generator mode shapes.
4. The mode shapes of the system with a sub-optimal output feedback STATCOM controller destroyed more states than the optimal STATCOM controller. The electromechanical

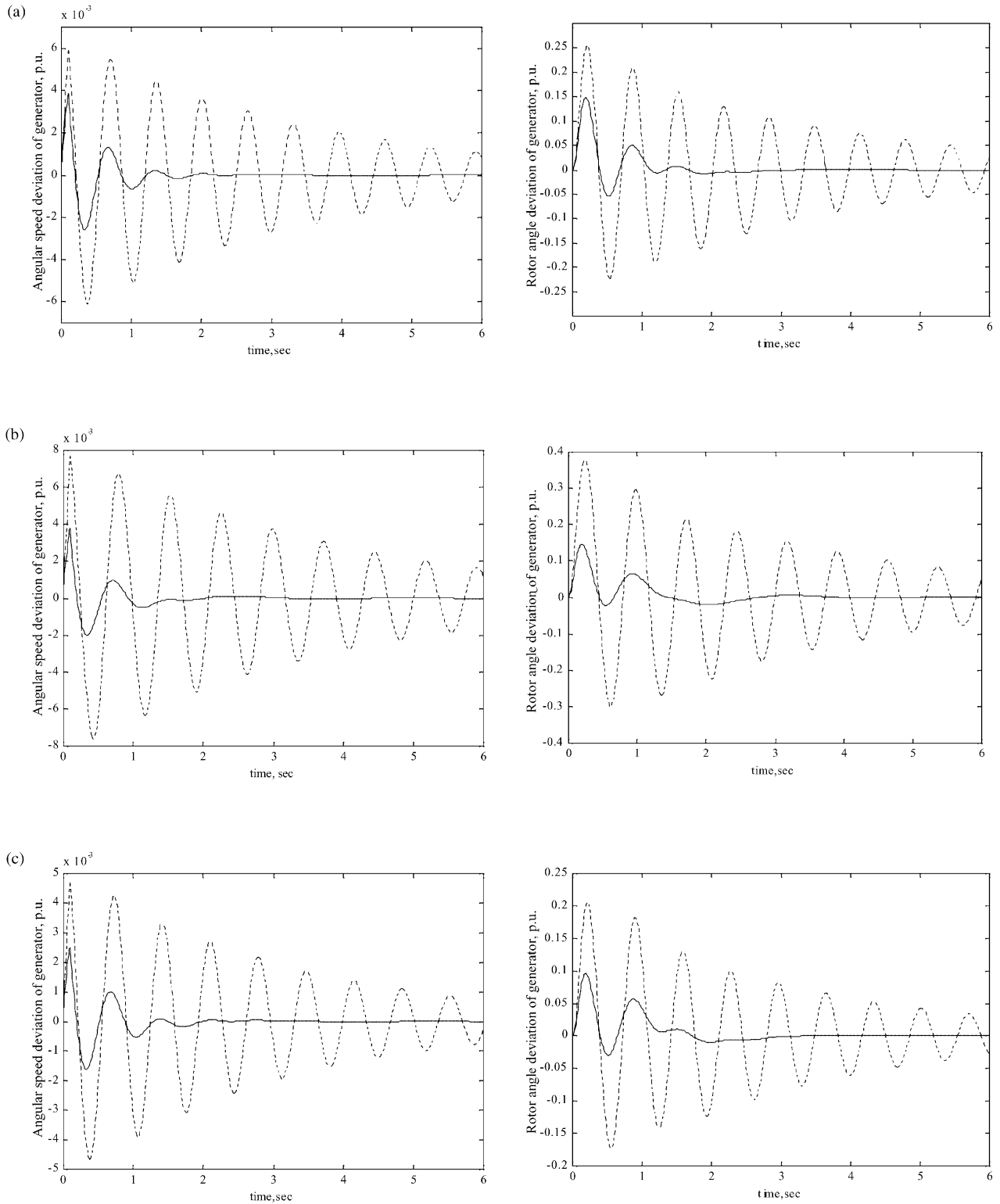


Fig. 9. Dynamic responses under different load conditions for 100 ms, line open-fault disturbance. (a) $P_0 = 1.0$, P.F. = 0.85 lag. (b) $P_0 = 1.2$, P.F. = 0.7 lag. (c) $P_0 = 0.8$, P.F. = 0.7 lag. ---: open system, —: system with STATCOM and output feedback controller (MEE).

and exciter mode damping were improved to an acceptable region.

5. Conclusions

In this paper, a systematic approach was used to design a STATCOM controller to damp the electromechanical mode oscillations in a power system. The state feedback gain of this controller was designed using the proposed LQR method, and does not involve choosing the weighting matrices. The output feedback gain was obtained using the direct and minimum error excitation methods. Eigenvalue analysis and dynamic simulations show that the proposed STATCOM controller can provide adequate electromechanical mode damping for a power system under disturbance. The decentralized STATCOM control, which is designed to increase the damping of the multimachine power system by the multiple constraint minimum error-excitation method, is currently under study and will be submitted later.

Acknowledgements

The author would like to thank the Fu-Jen Catholic University Cross-Cultural Center (0202-General-1999-1.0-0141) for the financial support to the study, and the Fu-Jen Catholic University and SVD section for the support of computing facilities.

Appendix A. System data

Generator and transmission line.

Rated 160 MVA, rated voltage 15 kV, power 1.0 p.u., power factor 0.85 lag, $X'_d = 0.265$ p.u., $X_d = 1.72$ p.u., $X_q = 1.66$ p.u., $R_a = 0.001296$ p.u., $D_g = 0.0$, $M_g = 4.74$ s, $T'_{q0} = 0.075$ s, $T'_{d0} = 5.90$ s, $\omega_b = 377$ rad s⁻¹, $R_{e1} = R_{e2} = 0.03$ p.u., $L_{e1} = L_{e2} = 0.6$ p.u., $R_{e3} = 0.05$ p.u., $L_{e3} = 0.05$ p.u.

Exciter. $K_A = 13.0$, $T_A = 0.21$ s, $K_F = 0.05$ s, $T_F = 1.0$ s, $K_E = -0.0497$, $T_E = 0.185$ s, $AEX = 0.0013$, $BEX = 0.553$

50% static load. $C_p = 0.25$, $C_q = 0.12$

Induction motor load [18].

Rated 1500 HP, rated voltage 2.3 kV, $R_s = 0.056$ Ω , $R_r = 0.037$ Ω , $L_s = 0.0537$ H, $L_r = 0.0537$ H, $M = 0.0527$ H, $J = 44.548$ kg m². 20 motors are used to represent 50% of dynamic load.

STATCOM unit [19]. $R'_s = 0.01$ p.u., $L' = 0.15$ p.u., $K = 4.0/\pi$, $C' = 0.85$ p.u., $R'_p = 100$ kp.u.⁻¹, $\theta_{d0} = 0^\circ$, $T_m = 0.024$ s, $K_m = 1.0$

Initial operating conditions. $P_0 = 1.0$ p.u., $V_t = 1.0$ p.u., $P.F. = 0.85$ lag.

References

- [1] Wang L, Tsai Z-Y, Liu L-S. Dynamic stability enhancement of parallel operated generators using STATCOM. Proceedings of the 19th Symposium on Electrical Power Engineering, 1998. p. 18–23.
- [2] Anderson PM, Fouad AA. Power system control and stability. Iowa State University Press, 1977.
- [3] Yan A, Yu YN. Multi-mode stabilization of torsional oscillations using output feedback excitation control. IEEE Trans PAS 1982;101(5):1245–53.
- [4] Putman TH, Ramey DG. Theory of the modulated reactance solution for subsynchronous resonance. IEEE Trans PAS 1992;101(6):1527–35.
- [5] Wasynczuk O. Damping subsynchronous resonance using reactive power control. IEEE Trans PAS 1981;100(3):1096–103.
- [6] Hammad AE, El-Sadek M. Application of a thyristor controlled var compensator for damping of subsynchronous oscillations in power system. IEEE Trans PAS 1984;103(1):198–212.
- [7] Hingorani NG. A new scheme for subsynchronous resonance damping of torsional oscillation and transient torques—part I. IEEE Trans PAS 1981;100(4):1852–5.
- [8] Irvani MR, Mathur RM. Damping of subsynchronous oscillations in power system using a static phase-shifter. IEEE Trans PWR 1986;1(2):76–83.
- [9] Wu C-J, Lee Y-S. Application of simultaneous active and reactive power modulation of superconducting magnetic energy storage unit to damp turbine generator subsynchronous oscillations. IEEE Trans EC 1993;8(1):63–70.
- [10] Lee Y-S. Superconducting magnetic energy storage controller design and stability analysis for a power system with various load characteristics. Elect Power Syst Res 1999;51:33–41.
- [11] Patil KV, Senthil J, Jiang J, Mathur RM. Application of STATCOM for damping torsional oscillations in series compensated AC systems. IEEE Trans EC 1998;13(3):237–43.
- [12] IEEE Committee Report. Computer representation of excitation system. IEEE Trans PAS 1968:50–4.
- [13] Lee WJ, Chen MC, Williams LB. Load model for stability studies. IEEE Trans IP 1987;23:159–65.
- [14] Choudary MA, Reza MA, Ellithy KA. Design of a robust modulation controller over a wide range of load characteristics for the AC/DC system. IEEE Trans Power Syst 1990;5:212–8.
- [15] Ellithy KA, Choudary MA. Effect of load models on the AC/DC system stability and modulation control design. IEEE Trans Power Syst 1988;4:411–8.
- [16] Hammam AE, El-Sadek MA. Prevention of transient voltage instability due to induction motor loads by static var compensators. IEEE Trans Power Syst 1984;9:1182–90.
- [17] Abledu KO, Mahmoud AA. Equivalent load model of induction machines. Elect Mach Power Syst 1984;9:435–52.
- [18] Cathey JJ, Cavin III RK, Ayoub AK. Transient load model of an induction motor. IEEE Trans Power Appar Syst 1973;92:1399–406.
- [19] Schauder CD, Mehta H. Vector analysis and control of advanced static var compensators. IEE Proc-C 1993;140(4):299–306.
- [20] Shieh LS, Dib HM, Mcinnis BC. Linear quadratic regulators with eigenvalue placement. IEEE Trans AC 1986;31(3):241–3.
- [21] Lee Y-S. To damp torsional oscillations of synchronous motor driving system with suboptimal control and strip eigenvalue placement. Proceedings of the IASTED International Conference, 2000. p. 499–502.